ISBN: 978-3-95450-184-7 doi:10.18429/JACoW-IPAC2018-MOPML008

JLEIC ELECTRON RING DYNAMIC APERTURE WITH NON-LINEAR FIELD ERRORS *†

Y. Nosochkov‡, Y. Cai, SLAC National Accelerator Laboratory, Menlo Park, CA, USA
F. Lin, V. S. Morozov, G. H. Wei, Y. Zhang, Jefferson Lab, Newport News, VA, USA

Abstract

We present results of dynamic aperture study for the updated electron ring lattice of the Jefferson Lab Electron-Ion Collider (JLEIC). The lattice design features low emittance arcs with local compensation of sextupole non-linear effects, and low emittance non-linear chromaticity correction sections. Dynamic aperture tracking simulations are performed to evaluate the effects of non-linear field errors, the sensitivity to betatron tune, and the impact of momentum error. Dynamic aperture is also evaluated with the measured PEP-II field errors. Preliminary tolerances to the non-linear field errors in the Final Focus quadrupoles are estimated.

INTRODUCTION

The design of the Jefferson Lab Electron-Ion Collider (JLEIC) [1] is based on a figure-8 layout, as shown in Fig. 1 for the electron ring. This special ring geometry provides an optimal preservation of the ion and electron polarization [2]. The 2.3-km electron and ion rings are housed in the same tunnel; they cross each other horizontally at the Interaction Point (IP), where $\beta_x^* = 10$ cm, $\beta_y^* = 2$ cm, and the crossing angle is 50 mrad. A second IP can be added in the other straight as a future upgrade. The machine is designed for a large range of collision beam energies: 3-12 GeV for electrons, 20-100 GeV for protons, and up to 40 GeV per nucleon for ions.

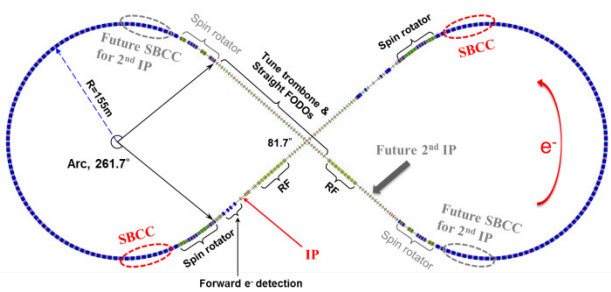

Figure 1: Layout of the JLEIC electron collider ring.

The electron ring consists of two arcs and two long straight sections. The straights include one Interaction Region (IR), spin rotator sections, RF-cavities, tune trombones, and a chicane for forward electron detection and polarimetry. A comparison study of various electron ring lattice options had been previously conducted [3] based on performance of chromaticity correction, dynamic aperture (DA), and beam emittance. The study concludes that the lattice, based on short-FODO arc cells, provides the best overall properties with an adequate non-linear chromaticity correction, maximum dynamic aperture (without errors), and sufficiently low emittance.

In this study, we use the updated short-FODO-cell lattice, and perform DA tracking simulations to evaluate the effects of non-linear field errors, the sensitivity to betatron tune, and the impact of momentum error. Preliminary tolerances to non-linear field errors in the Final Focus Quadrupoles (FFQ) are estimated. Dynamic aperture with the measured PEP-II field errors is also evaluated.

LATTICE

The optimal electron ring lattice [3] is based on short FODO arc cells, yielding the maximum DA (without errors), the low 5.7 nm-rad emittance at 5 GeV, and adequate non-linear chromaticity correction. The updated optics of this design is shown in Fig. 2, where the ring is 2.3 km long, and the tune is $\nu_{x,y} = 59.22, 59.16$. The low emittance is achieved using the short (11.4 m) arc cells with high phase advance (108°) per cell. This phase advance also provides conditions for cancellation of non-linear effects from the periodic arc sextupoles in every 10 cells [4] due to the multiple of 2π phase advance. For this reason, the two-family linear chromaticity sextupoles are included in 40 cells of each arc.

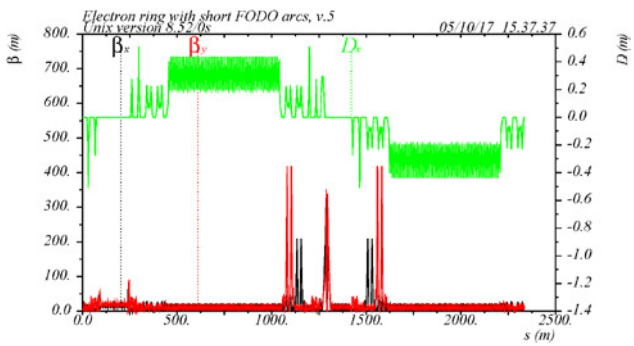

Figure 2: Optics functions of the electron collider ring, where IP is at s = 1292 m.

Another factor contributing to the low emittance is the optimized lattice of the non-linear Chromaticity Correction Block (CCB). This optics follows the SuperB design [5], and is called SBCC in this paper. Each SBCC consists of two non-interleaved *–I* pairs of sextupoles for X and Y correction, where the corresponding beta functions at the X and Y sextupoles are enlarged for the efficient correction, and the dipoles near the peaks of dispersion and β_x function are removed for the low emittance. The SBCC dipole lengths and the bending angles are further

* Work supported by the US DOE Contract DE-AC02-76SF00515.
† Authored by Jefferson Science Associates, LLC under US DOE Contract No. DE-AC05-06OR23177 and DE-AC02-06CH11357.
‡ yuri@slac.stanford.edu

ISBN: 978-3-95450-184-7 doi:10.18429/JACoW-IPAC2018-MOPML008

adjusted to guarantee the low emittance contribution. The optics of one SBCC is shown in Fig. 3, where the two *–I* sextupole pairs are near the four peaks of the beta functions.

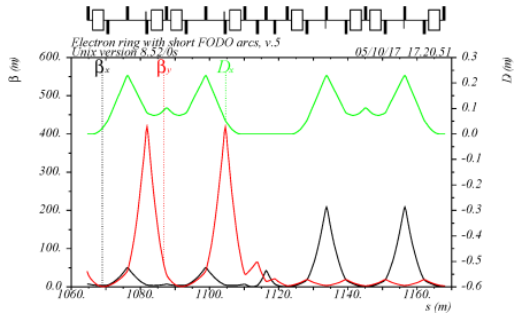

Figure 3: Optics of one SBCC section.

Four SBCC sections of the same design, but different beta functions, are included. Two high-β SBCCs are at the arc ends near the IP straight (as can be seen in Fig. 2) to correct the large non-linear chromaticity from the FFQ on each side of the IP. Phase advance between the SBCC and the IP in the correcting plane is set to near $\pi/2+n\pi$, fine-tuned for minimum variation of momentum dependent tune and β* as shown in Fig. 4. This correction provides more than $\pm 10\sigma_p$ of momentum range ($\sigma_p = 4.6 \cdot 10^{-4}$ at 5 GeV). Two low-β SBCCs are placed at the other arc ends; they are reserved for the future second IP, in which case they will be converted to high-β SBCCs by adjusting the quadrupole strengths.

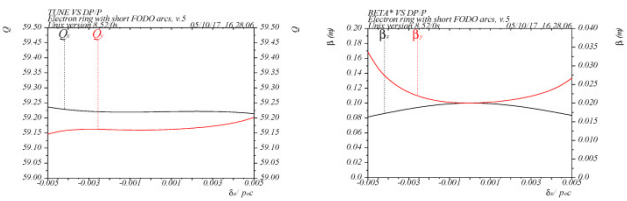

Figure 4: Tune (left) and β* (right) vs Δp/p.

DYNAMIC APERTURE

LEGO [6] code is used for the dynamic aperture calculations. The DA is calculated at the IP, using short-term tracking with 1024 turns, and expressed in units of the rms beam size (σ) for 5.7 nm-rad emittance at 5 GeV. The simulations are performed with and without momentum offset Δp/p, with synchrotron oscillations included. The RF voltage is 3.15 MV at 5 GeV. Linear chromaticity is always corrected to +1 using the two-family arc sextupoles, while the non-linear chromaticity is corrected using the high-β SBCC sextupoles. The effects of non-linear fringe field in dipoles and quadrupoles are included. The tracking is done for 21 angles in X-Y space and 10 seeds of random errors, from which the DA value is determined as the minimum DA among all the angles and the 10 seeds.

Dynamic aperture is verified with and without the non-linear fringe effects in quadrupoles and dipoles. The fringe field in quadrupoles creates octupole-like effects. These effects are significantly enhanced in the final focus quadrupoles due to the high beta functions, resulting in reduction of dynamic aperture as shown in Fig. 5. By default, we include the non-linear fringe effects in all the simulations.

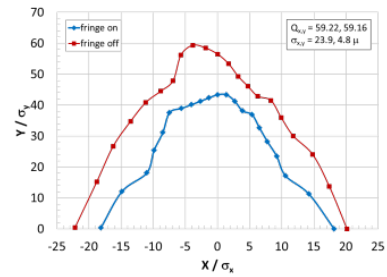

Figure 5: Dynamic aperture without errors, with (blue) and without (red) the non-linear fringe field effects.

The betatron tune used in this study is $\nu_{x,y}$ = 59.22, 59.16. It is optimized for a large momentum range. Figure 6 shows a sufficiently large dynamic aperture exceeding 10σ for the momentum error of up to $9\sigma_p$.

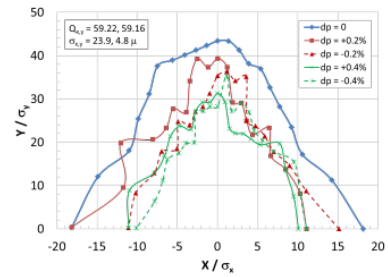

Figure 6: Dynamic aperture without errors vs Δp/p for $\nu_{x,y}$ = 59.22, 59.16.

The optimal tune with colliding beams will be determined by both the machine errors and the beam-beam effects. To verify sensitivity to the tune, we perform simulations at the different tune of $\nu_{x,y}$ = 59.53, 59.567. The tune near and above the high-integer, for example, was used in PEP-II operations [7]. The resulting dynamic aperture is shown in Fig. 7; it is comparable to the DA in Fig. 6, although the momentum range and the off-momentum DA are somewhat reduced. This is due to the close proximity to the half-integer resonances.

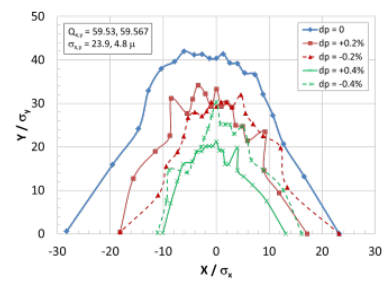

Figure 7: Dynamic aperture without errors vs Δp/p for $\nu_{x,y}$ = 59.53, 59.567.

DA with Non-Linear Field Errors

As a next step, we estimate the DA sensitivity to magnet non-linear field errors. Since the Field Quality (FQ) is

ISBN: 978-3-95450-184-7 doi:10.18429/JACoW-IPAC2018-MOPML008

not yet available for the electron ring magnets in this design, we use the measured FQ of PEP-II magnets [7]. The corresponding normal field systematic and random components are listed in Table 1. Dynamic aperture with these errors in all magnets for 10 random seeds is shown in Fig. 8. The minimum and average DA are 11σ and 13σ, respectively, which is acceptable. However, other types of errors and corrections are not yet included.

Table 1: PEP-II Measured Normal Field Components b_n at Reference Radius R in 10^{-3} Units

Dipole	**n**	**Systematic**	**Random**
R=30 mm	3	0.01	0.032
	4		0.032
	5		0.064
	6		0.082
Quadrupole	**n**	**Systematic**	**Random**
R=44.9 mm	3	1.03	0.56
	4	0.56	0.45
	5	0.48	0.19
	6	2.37	0.17
	10	-3.10	0.18
	14	-2.63	0.07
Sextupole	**n**	**Systematic**	**Random**
R=56.52 mm	9	-14.5	2.2
	15	-13.0	1.05

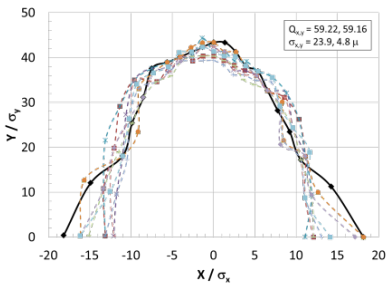

Figure 8: Dynamic aperture with PEP-II systematic and random field errors in all magnets for 10 random seeds (dash). The solid line is the DA without errors.

Tolerances to FFQ Systematic Field Errors

For the study of tolerances to the FFQ systematic non-linear field errors, we scan one FFQ systematic field component b_n at a time (n = 3, 4, 5, 6, 10), while the other FFQ components are turned off. The PEP-II systematic field errors in Table 1 are applied to all other magnets. The resulting dependence of DA on the systematic b_3, b_4, b_5 and b_6 is shown in Fig. 9. The "tolerances" are estimated by restricting the b_n to the same DA reduction (red dash lines in Fig. 9) for each multipole order; they are listed in Table 2.

These preliminary tolerances are larger than the PEP-II systematic errors in Table 1, except the b_4 and b_6. The latter may be due to sensitivity to the corresponding 4th and 6th order resonances near the $\nu_{x,y}$ = 59.22, 59.16.

Finally, we verify dynamic aperture with all the FFQ systematic errors from Table 2 and PEP-II systematic errors in other magnets. Figure 10 shows the comparison for three cases: 1) no errors, 2) PEP-II systematic errors in all magnets, but no FFQ errors, and 3) the same as in 2, but with the FFQ errors from Table 2. The impact of the FFQ tolerance errors is a reduction of the horizontal DA by a few σ's. The dynamic aperture is still sufficient. Note that some of the tolerances in Table 2 are quite loose. These values may be further optimized by making the loose tolerances somewhat tighter and the tight tolerances looser, which may be more practical while improving the dynamic aperture.

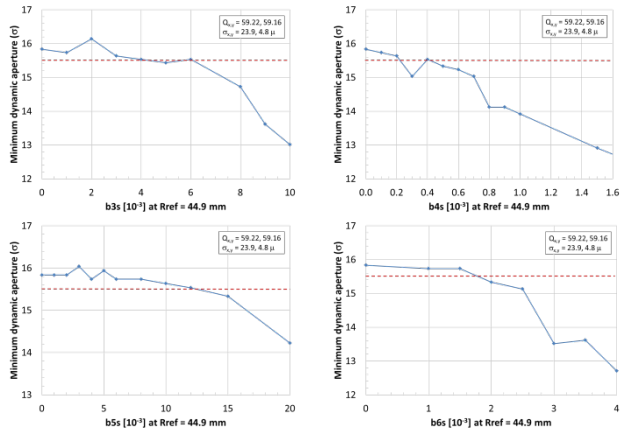

Figure 9: DA vs systematic b_3, b_4 (top) and b_5, b_6 (bottom) field components in the FFQ.

Table 2: Preliminary Tolerances to the FFQ Normal Systematic Field Errors, shown in 10^{-3} Units

b_{3s}	b_{4s}	b_{5s}	b_{6s}	b_{10s}
4	0.2	10	1.5	35

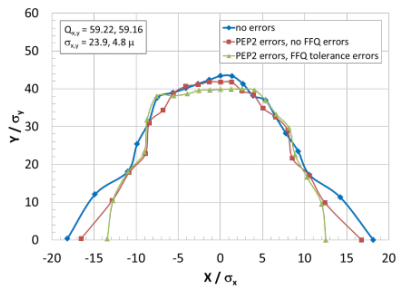

Figure 10: DA comparison: blue – no errors; red – PEP-II systematic field errors in quads and no FFQ errors; green – FFQ errors from Table 2 and PEP-II errors in other magnets.

CONCLUSION

The study of the JLEIC electron ring dynamic aperture shows that the DA of the short-FODO lattice provides a sufficiently large momentum range and is not very sensitive to the studied different working points. A more comprehensive tune scan is needed to determine the optimal tune with the best DA. Sensitivity to non-linear field errors is verified using the measured PEP-II field errors. The resulting dynamic aperture is sufficient. Preliminary tolerances to the FFQ systematic field errors are evaluated. The DA is sufficient, and may be further improved with more optimization of the specifications.

ISBN: 978-3-95450-184-7 doi:10.18429/JACoW-IPAC2018-MOPML008

REFERENCES

[1] S. Abeyratne *et al.*, "MEIC design summary", 2015, http://casa.jlab.org/MEICSumDoc1-2015/MEIC_Summary_Document_1-2015.pdf

[2] Ya. S. Derbenev, University of Michigan report UM HE 96-05, 1996.

[3] Y. M. Nosochkov, Y. Cai, M. K. Sullivan, Ya. S. Derbenev, F. Lin, V. S. Morozov, F. C. Pilat, G. H. Wei, Y. Zhang, M.-H. Wang, "Update on the JLEIC electron collider ring design", in *Proc. IPAC'2017*, paper WEPIK041, Copenhagen, Denmark, 2017.

[4] K. L. Brown, "A second-order magnetic optical achromat", SLAC-PUB-2257, 1979.

[5] M. Bona *et al.*, "SuperB: A high-luminosity asymmetric e^+ e^- super flavor factory. Conceptual design report.", INFN-AE-07-02, 2007.

[6] Y. Cai, M. Donald, J. Irwin, and Y. Yan, "LEGO: a modular accelerator design code", SLAC-PUB-7642, 1997.

[7] "PEP-II conceptual design report", SLAC-418, 1993.